

Sub  
A2 B4  
Cond. 24. (new) A semiconductor imaging device according to claim 19,  
further comprising:

a plurality of charge sensitive amplifiers respectively coupled to individuals of said plurality of pixels, said plurality of charge sensitive amplifiers and said plurality of pixels together comprising an active pixel image sensor.

#### REMARKS

The Examiner has objected to the specification as failing to show various labels in the drawings and for marking the drawings incorrectly with other labels. The applicant has amended the drawings and the specification accordingly. In particular, Fig. 1 has been amended to correspond to the labeling set forth in the specification and to include all layers mentioned. In addition, Fig. 2 has been amended to correspond to the labeling set forth in the specification, with the exception that layers 167 and 165 which correspond to Fig. 1 have been marked accordingly in Fig. 2 as would be understood by those skilled in the art. Fig. 2a has been broken out from Fig. 2 for purposes of clarity. Fig. 3 has likewise been amended to show the layers of Fig. 1 as would have been well understood by those skilled in the art. It is respectfully submitted that no new matter has been added.

The specification has been amended to refer to Fig. 2a separately. Further, on page 8, definitions of acronyms have been inserted for clarity. On pages 8-15, minor clarifications have been added to the specification for ease of reading, and on page 12, material taken from the original claims is incorporated into the specification. It is respectfully submitted that none of these clarifications add new matter as all would have been understood by those skilled in the art from the original text.

The Examiner has rejected the claims under 35 USC Section 112, first paragraph. According to the Examiner, the structure of the semiconductor imaging device (claim 1), charge coupled device (claim 2), active pixel structure (claim 3), 3-phase operation, etc. are not clearly described to enable any person skilled in the art to make and use the invention, and possible useful embodiments are not shown in the figures.

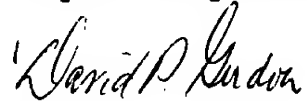
The applicant respectfully traverses the Examiner's rejection for the following reasons. It should be noted at the outset that the level of skill in the art for the art involved is extremely high. In addition, the structure of the semiconductor imaging device is indeed set forth in great detail in Figs. 1, 2, and 4, and its functioning is shown in Fig. 3. The entire specification teaches how to build such a device. As understood by the undersigned (who is not nearly skilled in the art), light which

impinges on the mesas will get absorbed in the storage region (the metal electrode preventing absorption in the barrier region). The mirror layers 151, 152 will cause light to reflect inside the semiconductor structure. Thus, each mesa structure and structure under that mesa acts as a pixel. The result of light being absorbed is that electrons will leave the quantum well layer 159 and be received in other layers. At the end of a cycle, the remaining charge in the quantum well of a pixel is (inversely) indicative of the amount of light absorbed. The charge may then be sequentially read out of the device by sequentially transferring the charge to an adjacent pixel (e.g., as a shift-register), and comparing at a last pixel the read out charge to a reference value. In this well known manner, a charge coupled device is established. This functioning is explained in the specification with respect to Fig. 4.

Claims 1-8 have been canceled as they were inartfully prepared by a pro-se applicant. New claims 9-24 have been substituted. It is respectfully submitted that the new claims are supported by the specification, and are allowable over the prior art.

In light of all of the above, it is submitted that the claims are in order for allowance, and prompt allowance is earnestly requested. Should any issues remain outstanding, the Examiner is invited to call the undersigned attorney of record so that the case may proceed expeditiously to allowance.

Respectfully submitted,

A handwritten signature in cursive script, appearing to read "David P. Gordon".

David P. Gordon  
Reg. #29,996  
Attorney for Applicant(s)

65 Woods End Road  
Stamford, CT 06905  
(203) 329-1160

Dec. 10, 2001

41 resonant cavity at the wavelength of interest in the LWIR or MWIR regions. In the described embodiment, ion implants are used for several purposes. The N type implant is used to form source and drain regions to the inversion channel, and it is also used to shift the threshold voltage of the inversion channel interface. The epitaxial structure is grown as a normally off (enhancement) device and then the N type implant is used to create regions of normally on (depletion) devices and it is these regions where the charge packets are stored. Oxygen implants may also be used to create high resistance regions below the implants. The technology utilizes the oxidation of AlAs and other layers with large aluminum percentages to achieve passivation, isolation and dielectric mirrors below the structure.

The basic structure of the pixel and the output amplifiers which are employed in the CCD may also be used to design an active pixel sensor. In such a design, each pixel is interfaced to an output amplifier and a row or a column is output in parallel.

#### BRIEF DESCRIPTION OF THE DRAWINGS

FIG.1 is a schematic view of the epitaxial layer structure indicating the modulation doped interface, the delta-doped resistively coupled layer and the delta-doped p contact layer

FIG.2 is a fabricated device cross-section of the CCD pixels including the pixel storage region, the pixel blocking region and the inter-pixel transfer region.

FIG. 2a is the potential profile of the device of Fig. 2.

FIG.3 is an energy diagram cross-section in the vertical direction through a storage pixel in the illuminated condition showing all of the significant current flows from the contacts and into and out of the well.

FIG.4 is schematic drawing of the last storage well in the CCD and its connection by way of a separate clocked-output gate to the output differential amplifier by way of a floating diffusion node which is reset each clock cycle. For the active pixel,  $V_\phi$  is the single storage element connected to the output stage.

## DESCRIPTION OF THE PREFERRED EMBODIMENTS

FIG.1 shows the epitaxial layer structure corresponding to the preferred embodiment and from which the CCD, the active pixel and the HFET (heterostructure field effect transistor) can be made. The layer structure starts from a semi-insulating GaAs substrate 100 and grows a DBR (distributed Bragg reflector) mirror stack of 1 - 3 pairs of 1/4 wavelength mirror using combinations of GaAs as layer 151 and AlAs as layers 152 which are subsequently oxidized to produce layers of  $Al_xO_y$  positioned between layers of GaAs. These layers form a bottom mirror for a cavity which is resonant at the intersubband wavelength of interest. Only a few pairs are used (1 - 3) to create a modest resonance in order to limit the total layer thickness and therefore epitaxial growth time. Following the DBR growth, a layer 170 of p+ GaAs of about  $0.5\mu m$  is grown to enable a bottom ohmic contact to the collector. Then a layer 171 of  $Al_{x1}Ga_{y1}As$  ( $0.4 < x1 < 1$ ), and where  $y1 = 1 - x1$ ) is grown to a thickness of about 1000-2000Å to assist

in the contact formation with a p type doping of about  $10^{18}\text{cm}^{-3}$ . and is followed by another layer 156 of undoped  $\text{Al}_{x1}\text{Ga}_{y1}\text{As}$  of about 1000-3000 Å to provide carrier confinement. This is followed by layer 157 of undoped  $\text{Al}_{x2}\text{Ga}_{y2}\text{As}$  ( $0.1 < x2 < 0.3$ ) and then a separation layer 158 of undoped GaAs. Layer 158 enables a growth interruption to lower the growth temperature for growing the quantum well(s). Layers 157 and 158 isolate the quantum wells from the carrier confinement layers 156. Next the undoped quantum well 160 and undoped barrier layer 159 are grown as a pair and there may be one to three pairs. The quantum well has been designed for intersubband absorption. A thin layer 161 of undoped GaAs of about 30 Å is then grown as a spacer which enables a growth temperature change between the InGaAs well and the layers above the well(s). The GaAs spacer is followed by an undoped spacer layer 162 of about 30 Å of  $\text{Al}_{x2}\text{Ga}_{y2}\text{As}$ . Then the modulation doped layer 163 of N+ type doped  $\text{Al}_{x2}\text{Ga}_{y2}\text{As}$  (where  $y2=1-x2$ ) is grown with a thickness of 40-100 Å to contain an ion density of  $10^{12}\text{cm}^{-2} < Q < 4 \times 10^{12}\text{cm}^{-2}$ . On top of the modulation doped layer is grown an undoped capacitor spacer layer 164 of 100-300 Å thickness which can be as thin as possible consistent with the growth and fabrication. On top of the capacitor layer is grown a P+ doped layer 165 which serves as the charge source layer for the gate. This layer should be as thin as possible and as highly doped as possible providing that it remains only partially depleted under all conditions of operation, i.e. a portion of this layer, however small, always remains undepleted. Above the charge source layer is grown a cladding layer 166 of thickness 500 Å  $< z < 2000$  Å, of doping in the range of  $10^{17}\text{cm}^{-3}$  and of composition  $\text{Al}_{x1}\text{Ga}_{y1}\text{As}$ . This layer serves to block minority carrier injection into the gate. The final

A1  
 Cont.

layer 167 is a GaAs layer of about 100 Å or thinner and with P<sup>++</sup> type doping which enables the formation of a very low resistance ohmic contact for hole carriers.

AI  
Conf.

The CCD is formed as a series of mesas 115 in Fig.2 and referred to as pixels, separated by regions 116 referred to as the inter-electrode transfer regions in Fig.2 . The mesas are created by patterning the original wafer (with photoresist for example) and then etching (typically by reactive ion etching for accuracy) to the charge source layer 165. Between the electrodes, an ion implant 121 is positioned so that the storage region 118 and the adjacent barrier region 117 of the next mesa are connected by a high conductivity region. This implant 121 is simultaneously used to form the source and drain regions of all transistors in the integrated circuit. Thus each storage region is connected to the next barrier region by a source implant. These inter-electrode regions are designed to maximize the drift current from pixel to pixel during charge transfer. Suppose that the voltage difference between clock phases is 2V and it is desired to achieve the maximum channel velocity corresponding to  $E=5 \times 10^3$  V/cm. Then an inter-electrode region width of 4μm would be desirable. The pixels are divided into a barrier region 117 and a storage region 118. The barrier region is contacted by the metal gate electrode 120 which is formed from a refractory metal such as tungsten or a tungsten alloy and produces an ohmic contact with the topmost GaAs layer 167. The gate electrode is formed upon the as-grown epitaxial material which has an enhancement threshold meaning that it is in the off condition with zero gate voltage. The storage region is adjacent to the barrier region and is defined with an ion implant 119 of N type species into the active layer. Therefore, the region of the mesa without the implant, defines the barrier region. The purpose of the



implant is to move the threshold of the interface to a normally on condition so that the potential profile under the gate electrode appears as shown in Fig. 2a. The metal emitter (gate electrode 120) is patterned to be approximately positioned over the barrier portion and to be equal to or greater than the barrier length. It is self-aligned to the left edge of the mesa. However, the P++ GaAs layer 167 is low enough in resistance to force the entire surface of the mesa to be at the potential of the metal electrode for all the current densities of interest in the operation. The storage section of the pixel is therefore at a constant potential along its length y in Fig.2 and this means the storage section is an equipotential region. The operation of this CCD is 1 1/2 phase which means that alternate electrodes are clocked to a voltage  $V_{\phi}$  and the other electrodes are held at a dc potential  $V_{dc}$ . The potential profiles under the clocked electrode and the dc electrode are shown in Fig. 2a, which illustrates the transfer mechanism. The voltage difference  $\Delta V = V_{\phi} - V_{dc}$  is applied to the resistor consisting of the P+ layer 165 between the mesas (i.e., in the inter-electrode region). The length of the resistor is chosen to maximize the velocity in the interelectrode transfer region. The maximum velocity therefore maximizes the current flow which is given by  $J = qvn$ , where  $v$  is the carrier velocity,  $q$  is the electronic charge and  $n$  is the carrier density. To optimize the transfer efficiency, it is necessary to maximize the current flow. This is achieved with the maximum value of  $v$  and the maximum value of  $n$ . The maximum value of  $v$  is obtained as just discussed and the maximum value of  $n$  is obtained by the implanted N+ region between electrodes as discussed above.

A1  
Cont.

AI  
Cont.

The scheme just discussed is a 1 1/2 phase clocking scheme. As is well known in Si technology, there are many possible clocking schemes and these may also be implemented here. These include a) a three phase clocking scheme wherein every third pixel is clocked with a phase I clock, the adjacent pixels to every third pixel are clocked with a phase II clock and the remaining pixels are clocked with a phase III clock, b) a fully two phase clocking scheme wherein every other pixel is clocked with a phase I clock and the remaining pixels are clocked with a phase II clock, and c) a uni-phase clocking scheme. The uni-phase clocking scheme is usually referred to as a virtual phase CCD and is achieved with a series of strategically placed p and n implants. The uni-phase operation has been exploited successfully in Si CCD's which use a buried electron channel to store the charge. The surface of the buried channel is inverted by voltage to produce a hole inversion channel which clamps the potential of the electron channel. This natural clamping of the surface potential by the formation of a p channel eliminates the need for a separate dc electrode allowing a single electrode to be used. The voltage at which this clamping occurs is controlled locally with a p type implant. All of these clocking schemes are applicable to the Inversion Channel GaAs CCD.

The CCD described above has the unique capability of detecting an input signal in the spectral range from about  $3\mu\text{m}$  to  $20\mu\text{m}$  by the mechanism of intersubband absorption. The energy band diagram of the device is shown in Fig.3 . It shows the quantum well and the current flows of charge carriers which may either fill the well or empty the well. The current flows into the well are the thermal emission from the modulation doped layer 161 to the left of the well, and the generation currents flowing

toward the well(s) from the collector depletion layer consisting of the layers 170,  
 171, 156, and 157 and from the quantum well(s) and barrier(s) which are layers 159 and  
 160 respectively. The currents flowing out of the well are the thermal emission current  
 from the quantum well into the modulation doped layer 163 and the photocurrent from  
 the quantum well into the modulation doped layer produced by the intersubband  
 absorption in the quantum well. The other important current flow is the recombination  
 current  $J_{rb}$  which allows electrons to flow from the modulation doped layer to the emitter  
 contact (metal gate electrode 120) via electron-hole recombination current in the  
 9 capacitor layer 164. During the operation as a photodetector, the emitter is forward biased  
 10 with respect to the collector (156, 157, 170, 171). This means that the capacitor layer 164  
 is forward biased and the collector layer is reverse biased which enables the photocurrent  
 to be conducted out of the system by forward bias and the dark current current flow  
 ( $J_{rbd}$ ) in the system to be controlled by the reverse bias across the collector. The  
 operation of the photodetector is described as follows. The quantum well is initially filled  
 substantially in the absence of light. A reasonable design is that the Fermi energy is  
 above the first subband in the quantum well. Then the absorption will be maximized  
 because it is proportional to the number of electrons in the initial state. When long  
 wavelength light is incident, then the photocurrent empties the quantum well. The dark  
 current flowing into the well is produced by the generation current which is produced by  
 emission across the energy gap of the quantum well or the barrier regions. The noise  
 current  $i_n$  in the device which represents the limit to the detectable power is specified by  
 the dark current  $I_d$  and it is

$$i_n^2 = 2qI_dB$$

where  $q$  is the electronic charge and  $B$  is the bandwidth. In a conventional QWIP device, the dark current flows over a small barrier of a size comparable to the quantum well and therefore to obtain high background limited operation, it is necessary to cool the device to cryogenic temperatures of 50-60K in order to reduce  $I_d$ . Only at these temperatures can the shot noise associated with the dark current be reduced to a level that is comparable to the noise associated with the black body radiation from the scene at a temperature of 300K.

AI  
cont.

The structure illustrated in Figs. 1-3 has a fundamental advantage in reducing the dark current flow even at temperatures up to and above 300K. The reason is that the barrier to the generation of dark current and the barrier to the optical emission from the quantum well are distinctly different. As the diagram shows, the dark current is produced by the thermal emission across the energy gap of either the quantum well (corresponding to strained InGaAs with a bandgap of about 1.24eV), the barrier region (corresponding to GaAs with a bandgap of 1.42eV), and the depletion regions (corresponding to  $Al_{x_2}Ga_{y_2}As$  with a bandgap of 1.65eV). Generally speaking the depletion regions become the main source of dark current. In contrast to the dark current barrier, the optical emission barrier is the energy interval between the first subband in the quantum well and the top of the well (this is basically the depth of the quantum well). Because this structure has decoupled the dark current generation barrier from the optical emission barrier, then it is possible to operate at room temperature and still achieve BLIP operation. Therefore we may realize all of the benefits of high resolution and high speed photovoltaic sensing offered by the QWIP detection mechanism with an uncooled semiconductor chip.

A1  
cont.

The infrared detection mechanism described above has been described as an integral part of an efficient CCD structure in GaAs. However the detector could equally as well be incorporated into the photo-sensitive portion of an active pixel structure. In the active pixel, the charge is transferred across one barrier to a bit line which connects to the sense amplifier. The charge transfer mechanisms are identical to those of the CCD, but the charge transfer efficiency is much less of an issue because there is only one transfer gate separating the storage area from the sensing node. The tradeoff is that the fill factor of the active pixel is less than the CCD because more circuitry is required. Therefore the operation of the intersubband detector is identical in the CCD and active pixel architectures.

In both the CCD and the active pixel devices, the signal of interest is actually the charge that is removed from the well. For very weak optical input signals, very little charge is removed and for very strong optical inputs the well is essentially emptied at the end of the imaging cycle. The situation is ideal for the elimination of noise in the detection process because it requires differential operation to obtain the actual output signal. For example, if the output of the imaged pixel is input to one side of a differential amplifier, then it is appropriate to input a signal to the other side of the DA from a full well to perform as a reference level. These connections are illustrated in Fig.4 which shows a storage gate  $V_\phi$ , a transfer gate  $V_{dc}$ , a reset gate  $V_{reset}$ , a differential amplifier and two reference nodes, one for a full well and one for an empty well. This situation is identical to that used in the correlated double sampling scheme in advanced CCD read-out circuits to reduce set:reset noise. There are several noise mechanisms contributing noise to the amplifier inputs which include clocking noise, kTC noise on the reset

transistor, and shot noise on the dark current to mention a few. All of the noise mechanisms that are common to the read-out of the cell with and without data, are reduced by the common mode rejection ratio of the differential amplifier. Therefore the intersubband detection within the inversion channel has a fundamental advantage because the differential process is essential to recover the signal, and yet at the same time, it performs the role of reducing many noise mechanisms according to the differential rejection of common mode signals

---

resonant cavity at the wavelength of interest in the LWIR or MWIR regions. In the described embodiment, ion implants are used for several purposes. The N type implant is used to form source and drain regions to the inversion channel, and it is also used to shift the threshold voltage of the inversion channel interface. The epitaxial structure is grown as a normally off (enhancement) device and then the N type implant is used to create regions of normally on (depletion) devices and it is these regions where the charge packets are stored. Oxygen implants may also be used to create high resistance regions below the implants. The technology utilizes the oxidation of AlAs and other layers with large aluminum percentages to achieve passivation, isolation and dielectric mirrors below the structure.

The basic structure of the pixel and the output amplifiers which are employed in the CCD may also be used to design an active pixel sensor. In such a design, each pixel is interfaced to an output amplifier. The output of the amplifier is output in parallel.

*marked-up  
pages*

B

IE DRAWINGS

FIG.1 is a schematic view of the epitaxial layer structure indicating the modulation doped interface, the delta-doped resistively coupled layer and the delta-doped p contact layer

FIG.2 is a fabricated device cross-section of the CCD pixels including the pixel storage region, the pixel blocking region and the inter-pixel transfer region.

FIG. 2a is the potential profile of the device of Fig. 2.

FIG.3 is an energy diagram cross-section in the vertical direction through a storage pixel in the illuminated condition showing all of the significant current flows from the contacts and into and out of the well.

FIG.4 is schematic [drwaing] drawing of the last storage well in the CCD and its connection by way of a separate clocked output gate to the output differential amplifier by way of a floating diffusion node which is reset each clock cycle. For the active pixel,  $V_{\phi}$  is the single storage element connected to the output stage.

## DESCRIPTION OF THE PREFERRED EMBODIMENTS

FIG.1 shows the epitaxial layer structure corresponding to the preferred embodiment and from which the CCD, the active pixel and the HFET (heterostructure field effect transistor) can be made. The layer structure starts from a semi-insulating GaAs substrate 100 and grows a DBR (distributed Bragg reflector) mirror stack of 1 - 3 pairs of 1/4 wavelength mirror using combinations of GaAs as layer 151 and AlAs as layers 152 which are subsequently oxidized to produce layers of  $Al_xO_y$  positioned between layers of GaAs. These layers form a bottom mirror for a cavity which is resonant at the intersubband wavelength of interest. Only a few pairs are used (1 - 3) to create a modest resonance in order to limit the total layer thickness and therefore epitaxial growth time. Following the DBR growth, a layer 170 of p+ GaAs of about  $0.5\mu m$  is grown to enable a bottom ohmic contact to the collector. Then a layer 171 of  $Al_{x1}Ga_{y1}As$  [ $(1 < x1 < 0.4)$  ( $0.4 < x1 < 1$ ), and where  $y1 = 1 - x1$ ] is grown to a thickness of about 1000-



2000 Å to assist in the contact formation with a p type doping of about  $10^{18} \text{ cm}^{-3}$  and is followed by another layer 156 of undoped  $\text{Al}_{x1}\text{Ga}_{y1}\text{As}$  of about 1000-3000 Å to provide carrier confinement. This is followed by layer 157 of undoped  $\text{Al}_{x2}\text{Ga}_{y2}\text{As}$   $[(0.3 < y1 < 0.1)]$   $(0.1 < x2 < 0.3)$  and then a separation layer 158 of undoped GaAs. Layer 158 enables a growth interruption to lower the growth temperature for growing the quantum well(s). Layers 157 and 158 isolate the quantum wells from the carrier confinement layers 156. Next the undoped quantum well 160 and undoped barrier layer 159 are grown as a pair and there may be one to three pairs. The quantum well has been designed for intersubband absorption. A thin layer 161 of undoped GaAs of about 30 Å is then grown as a spacer which enables a growth temperature change between the InGaAs well and the layers above the well(s). The GaAs spacer is followed by an undoped spacer layer 162 of about 30 Å of  $\text{Al}_{x2}\text{Ga}_{y2}\text{As}$ . Then the modulation doped layer 163 of N+ type doped  $\text{Al}_{x2}\text{Ga}_{y2}\text{As}$  (where  $y2=1-x2$ ) is grown with a thickness of 40-100 Å to contain an ion density of  $10^{12} \text{ cm}^{-2} < Q < 4 \times 10^{12} \text{ cm}^{-2}$ . On top of the modulation doped layer is grown an undoped capacitor spacer layer 164 of 100-300 Å thickness which can be as thin as possible consistent with the growth and fabrication. On top of the capacitor layer is grown a P+ doped layer 165 which serves as the charge source layer for the gate. This layer should be as thin as possible and as highly doped as possible providing that it remains only partially depleted under all conditions of operation, i.e. a portion of this layer, however small, always remains undepleted. Above the charge source layer is grown a cladding layer 166 of thickness 500 Å  $< z < 2000$  Å, of doping in the range of  $10^{17} \text{ cm}^{-3}$  and of composition  $\text{Al}_{x1}\text{Ga}_{y1}\text{As}$ . This layer serves to block minority carrier injection into the gate. The final layer 167 is a GaAs layer of about 100 Å or

thinner and with P<sup>++</sup> type doping which enables the formation of a very low resistance ohmic contact for hole carriers.

The CCD is formed as a series of mesas 115 in Fig.2 and referred to as pixels, separated by regions 116 referred to as the inter-electrode transfer regions in Fig.2 . The mesas are created by patterning the original wafer (with photoresist for example) and then etching (typically by reactive ion etching for accuracy) to the charge source layer 165. Between the electrodes, an ion implant 121 is positioned so that the storage region 118 and the adjacent barrier region 117 of the next mesa are connected by a high conductivity region. This implant 121 is simultaneously used to form the source and drain regions of all transistors in the integrated circuit. Thus each storage region is connected to the next barrier region by a source implant. These inter-electrode regions are designed to maximize the drift current from pixel to pixel during charge transfer. Suppose that the voltage difference between clock phases is 2V and it is desired to achieve the maximum channel velocity corresponding to  $E=5 \times 10^3$  V/cm. Then an inter-electrode region width of 4 $\mu$ m would be desirable. The pixels are divided into a barrier region 117 and a storage region 118. The barrier region is contacted by the metal gate electrode 120 which is formed from a refractory metal such as tungsten or a tungsten alloy and produces an ohmic contact with the topmost GaAs layer [114] 167. The gate electrode is formed upon the as-grown epitaxial material which has an enhancement threshold meaning that it is in the off condition with zero gate voltage. The storage region is adjacent to the barrier region and is defined with an ion implant 119 of N type species into the active layer. Therefore, the region of the mesa without the implant, defines the barrier region. The

purpose of the implant is to move the threshold of the interface to a normally on condition so that the potential profile under the gate electrode appears as shown in Fig.[3] 2a. The metal emitter (gate electrode 120) is patterned to be approximately positioned over the barrier portion and to be equal to or greater than the barrier length. It is self-aligned to the left edge of the mesa. However, the P<sup>++</sup> GaAs layer [114] 167 is low enough in resistance to force the entire surface of the mesa to be at the potential of the metal electrode for all the current densities of interest in the operation. The storage section of the pixel is therefore at a constant potential along its length y in Fig.2 and this means the storage section is an equipotential region. The operation of this CCD is 1 \_ phase which means that alternate electrodes are clocked to a voltage  $V\phi$  and the other electrodes are held at a dc potential  $V_{dc}$ . The potential profiles under the clocked electrode and the dc electrode are shown in Fig.[3] 2a, which illustrates the transfer mechanism. The voltage difference  $\Delta V = V\phi - V_{dc}$  is applied to the resistor consisting of the P<sup>+</sup> layer [112] 165 between the mesas (i.e., in the inter-electrode region). The length of the resistor is chosen to maximize the velocity in the interelectrode transfer region. The maximum velocity therefore maximizes the current flow which is given by  $J = qvn$ , where v is the carrier velocity, q is the electronic charge and n is the carrier density. To optimize the transfer efficiency, it is necessary to maximize the current flow. This is achieved with the maximum value of v and the maximum value of n. The maximum value of v is obtained as just discussed and the maximum value of n is obtained by the implanted N<sup>+</sup> region between electrodes as discussed above.

The scheme just discussed is a 1 1/2 phase clocking scheme. As is well known in Si technology, there are many possible clocking schemes and these may also be implemented here. These include a) a three phase clocking scheme wherein every third pixel is clocked with a phase I clock, the adjacent pixels to every third pixel are clocked with a phase II clock and the remaining pixels are clocked with a phase III clock, b) a fully two phase clocking scheme wherein every other pixel is clocked with a phase I clock and the remaining pixels are clocked with a phase II clock, and c) a uni-phase clocking scheme. The uni-phase clocking scheme is usually referred to as a virtual phase CCD and is achieved with a series of p and n implants. The uni-phase operation has been exploited successfully in Si CCD's which use a buried electron channel to store the charge. The surface of the buried channel is inverted by voltage to produce a hole inversion channel which clamps the potential of the electron channel. This natural clamping of the surface potential by the formation of a p channel eliminates the need for a separate dc electrode allowing a single electrode to be used. The voltage at which this clamping occurs is controlled locally with a p type implant. All of these clocking schemes are applicable to the Inversion Channel GaAs CCD.

The CCD described above has the unique capability of detecting an input signal in the spectral range from about 3 $\mu$ m to 20 $\mu$ m by the mechanism of intersubband absorption. The energy band diagram of the device is shown in Fig.3 . It shows the quantum well and the current flows of charge carriers which may either fill the well or empty the well. The current flows into the well are the thermal emission from the modulation doped layer [110] 161 to the left of the well, and the generation currents

flowing toward the well(s) from the collector depletion layer consisting of the layers [104, 105, 106, and 107] 170, 171, 156, and 157 and from the quantum well(s) and barrier(s) which are layers [108 and 109] 159 and 160 respectively. The currents flowing out of the well are the thermal emission current from the quantum well into the modulation doped layer [112] 163 and the photocurrent from the quantum well into the modulation doped layer produced by the intersubband absorption in the quantum well. The other important current flow is the recombination current  $J_{rb}$  which allows electrons to flow from the modulation doped layer to the emitter contact (metal gate electrode 120) via electron-hole recombination current in the capacitor layer [113] 164. During the operation as a photodetector, the emitter is forward biased with respect to the collector (156, 157, 170, 171). This means that the capacitor layer 164 is forward biased and the collector layer is reverse biased which enables the photocurrent to be conducted out of the system by forward bias and the dark current current flow ( $J_{rbd}$ ) in the system to be controlled by the reverse bias across the collector. The operation of the photodetector is described as follows. The quantum well is initially filled substantially in the absence of light. A reasonable design is that the Fermi energy is above the first subband in the quantum well. Then the absorption will be maximized because it is proportional to the number of electrons in the initial state. When long wavelength light is incident, then the photocurrent empties the quantum well. The dark current flowing into the well is produced by the generation current which is produced by emission across the energy gap of the quantum well or the barrier regions. The noise current  $i_n$  in the device which represents the limit to the detectable power is specified by the dark current  $I_d$  and it is

$$i_n^2 = 2qI_dB$$

where  $q$  is the electronic charge and  $B$  is the bandwidth. In a conventional QWIP device, the dark current flows over a small barrier of a size comparable to the quantum well and therefore to obtain high background limited operation, it is necessary to cool the device to cryogenic temperatures of 50-60K in order to reduce  $I_d$ . Only at these temperatures can the shot noise associated with the dark current be reduced to a level that is comparable to the noise associated with the black body radiation from the scene at a temperature of 300K.

The structure illustrated in Figs. 1-3 has a fundamental advantage in reducing the dark current flow even at temperatures up to and above 300K. The reason is that the barrier to the generation of dark current and the barrier to the optical emission from the quantum well are distinctly different. As the diagram shows, the dark current is produced by the thermal emission across the energy gap of either the quantum well (corresponding to strained InGaAs with a bandgap of about 1.24eV), the barrier region (corresponding to GaAs with a bandgap of 1.42eV), and the depletion regions (corresponding to  $\text{Al}_{x_2}\text{Ga}_{y_2}\text{As}$  with a bandgap of 1.65eV). Generally speaking the depletion regions become the main source of dark current. In contrast to the dark current barrier, the optical emission barrier is the energy interval between the first subband in the quantum well and the top of the well (this is basically the depth of the quantum well). Because this structure has decoupled the dark current generation barrier from the optical emission barrier, then it is possible to operate at room temperature and still achieve BLIP operation. Therefore we may realize all of the benefits of high resolution and high speed photovoltaic sensing offered by the QWIP detection mechanism with an uncooled semiconductor chip.

The infrared detection mechanism described above has been described as an integral part of an efficient CCD structure in GaAs. However the detector could equally as well be incorporated into the photo-sensitive portion of an active pixel structure. In the active pixel, the charge is transferred across one barrier to a bit line which connects to the sense amplifier. The charge transfer mechanisms are identical to those of the CCD, but the charge transfer efficiency is much less of an issue because there is only one transfer gate separating the storage area from the sensing node. The tradeoff is that the fill factor of the active pixel is less than the CCD because more circuitry is required. Therefore the operation of the intersubband detector is identical in the CCD and active pixel architectures.

In both the CCD and the active pixel devices, the signal of interest is actually the charge that is removed from the well. For very weak optical input signals, very little charge is removed and for very strong optical inputs the well is essentially emptied at the end of the imaging cycle. The situation is ideal for the elimination of noise in the detection process because it requires differential operation to obtain the actual output signal. For example, if the output of the imaged pixel is input to one side of a differential amplifier, then it is appropriate to input a signal to the other side of the DA from a full well to perform as a reference level. These connections are illustrated in Fig.4 which shows a storage gate  $V_\phi$ , a transfer gate  $V_{dc}$ , a reset gate  $V_{reset}$ , a differential amplifier and two reference nodes, one for a full well and one for an empty well. This situation is identical to that used in the correlated double sampling scheme in advanced CCD read-out circuits to reduce set:reset noise. There are several noise mechanisms contributing noise to the amplifier inputs which include clocking noise, kTC noise on the reset

transistor, and shot noise on the dark current to mention a few. All of the noise mechanisms that are common to the read-out of the cell with and without data, are reduced by the common mode rejection ratio of the differential amplifier. Therefore the intersubband detection within the inversion channel has a fundamental advantage because the differential process is essential to recover the signal, and yet at the same time, it performs the role of reducing many noise mechanisms according to the differential rejection of common mode signals